

HH137 and 138: discovering new knots and a molecular outflow with Gemini and APEX

Ferrero, L. V.^{1,2}, Cappa, C. E.^{2,3,4}, Gómez, M.^{1,2}, Saldaño, H. P.^{1,2}, Gunthardt, G.¹ and Rubio, M.⁵

¹ Observatorio Astronómico de Córdoba, Universidad Nacional de Córdoba, Argentina

² CONICET, Consejo Nacional de Investigaciones Científicas y Técnicas, Argentina

³ IAR, CCT - La Plata, CONICET and FCAG, UNLP, Argentina

⁴ Facultad de Ciencias Astronómicas y Geofísicas, Universidad Nacional de La Plata, Argentina

⁵ Departamento de Astronomía, Universidad de Chile, Chile

Introduction

Stellar jets appear during the initial stages of star formation where the incipient star begins to eject winds along the rotation axis. In the optical, these outflows appear as jets and/or Herbig-Haro (HH) objects, in the NIR as H_2 (2.12 μm) knots, and in the radio range as molecular outflows.

In particular, the H_2 line at 2.12 μm is a well-known shock or impact tracer, where the relatively hot material hits the cold molecular cloud environment, producing the molecular outflows detected at radio wavelengths.

Here, we present a study of HH 137 and HH 138, located in the dark nebula D291.4–0.2, at 2.2 kpc (Hartley et al. 1986), in the Carina region. These HH objects were identified by Ogura (1993), in [S II], H α , and [N II] lines, and show a chain of knots with typical emission of Herbig-Haro objects (their positions are indicated in Figure 1 with capital letters). At 2.2 kpc HH 137 and HH 138 are 0.84 pc and 0.23 pc long, respectively (Targon et al. 2011). Ogura (1993) suggests that the driving source should be located between HH 137-knot J and HH 138-knot A. However, it is not clear if HH 138 and HH 137 are linked by the same unknown driving source.

In this contribution, we search for NIR and radio counterparts of these jets using H_2 and K images obtained with Gemini South and molecular spectra taken with the APEX telescope. Our aims are to investigate the presence of molecular outflows and to analyze the molecular environment linked to the HH objects.

Gemini results

Figure 1 shows a composite image of HH 137 and HH 138 in K (blue), H_2 (green) and 4.5 μm (red). The chain of knots is seen in shock excited H_2 emission. The high angular resolution obtained with GSAOI+GeMS/Gemini reveals the internal structure of the knots in HH 137, which ends in a “bow-shock” structure. Some of them coincide with the optical knots positions but others, such as the H knot, are displaced.

The emission at 4.5 μm shows a striking arc-like structure, located between HH 137 and HH 138, not previously reported, indicated in the same figure. The 4.5 μm *Spitzer* band contains several lines or bands, as well as the shock-diagnostic rovibrational H_2 and CO lines (Reach et al. 2006; Smith & Rosen 2005; Watson et al. 2010).

The driving source

Tóth et al. (2014) identified a candidate young stellar object (YSO) in the AKARI/FIS young stellar objects catalog located at Ra,Dec(J2000) = (11:14:6.1,−60:52:59), close to the arc-like structure, coincident with the point source WISE J111406.96-605255.9 and with a *Spitzer* source (indicated in Figure 1).

Our analysis of the WISE source indicates a Class II object (Koenig et al. 2012). Its YSO status and its position near the arc detected at 4.5 μm and on the axis of HH 137 suggest that it may be powering the HH objects.

APEX results: An outflow linked to HH 137

Figure 2 shows an overlay of the $^{12}\text{CO}(3-2)$ emission distribution within the velocity interval $[-13.3, -8.4]$ km s^{-1} (in contours) and the H_2 and 4.5 μm images (in color scales). The CO image reveals molecular material coincident with HH 137, detected from the position of the proposed driving source up to the location of the bow-shock seen in H_2 . Their characteristics are consistent with a molecular outflow linked to HH 137 traced by CO.

The inset in this figure shows the $^{12}\text{CO}(3-2)$, $^{13}\text{CO}(3-2)$, and $\text{C}^{18}\text{O}(3-2)$ spectra averaged within the emitting region. The profiles display characteristics typical of outflows, i.e., an extended wing toward negative velocities with two maxima separated by an absorption dip in the optically thick $^{12}\text{CO}(3-2)$ line and only one maximum centered at the velocity of the absorption dip in the optically thin $\text{C}^{18}\text{O}(3-2)$ line (Chen et al. 2010; Bronfman et al. 2008). The fact that the red-shifted peak is brighter than the blue-shifted one, is indicative of outflow.

Bearing in mind the adopted system velocity of -6 km s^{-1} (as suggested by the $\text{C}^{18}\text{O}(3-2)$ and $\text{HCO}^+(3-2)$ line emissions), the ^{12}CO emission corresponds to the blue-shifted lobe of the outflow, which probably flows through a low-density region. Neither a red-shifted lobe nor emission linked to HH 138 was detected. We believe that the knots and the blue-shift outflow lie close to the plane of the sky. The main parameters of the outflow as derived following Beuther et al. (2002) and Buckle et al. (2010) are summarized in Table 1.

APEX results: The molecular clump

Figure 2 also shows the central part of a massive ($340 M_\odot$) and dense ($n_{\text{H}_2} = 9.4 \times 10^4 \text{ cm}^{-3}$) molecular clump centered at Ra,Dec(J2000) = (11:14:10,−60:53:00) of about $28'' \times 56''$ in size (0.3×0.6 pc at 2.2 kpc), detected in the velocity interval $[-22, +2]$ km s^{-1} in CO and $[-9.6, -3.3]$ km s^{-1} in HCO^+ . The arc at 4.5 μm coincides with the high-density border of this massive clump.

Figure 3 displays the $\text{HCO}^+(3-2)$ line and the cold dust continuum emission at 870 μm from the ATLASGAL (Schuller et al. 2009; Csengeri et al. 2014), where the clump is clearly identified. The brightest part of the dust emission coincides with the powering source and the 4.5 μm arc.

The detection of $\text{HCO}^+(3-2)$ is consistent with volume densities $n_{\text{H}_2} = 10^9 \text{ cm}^{-3}$ (critical density).

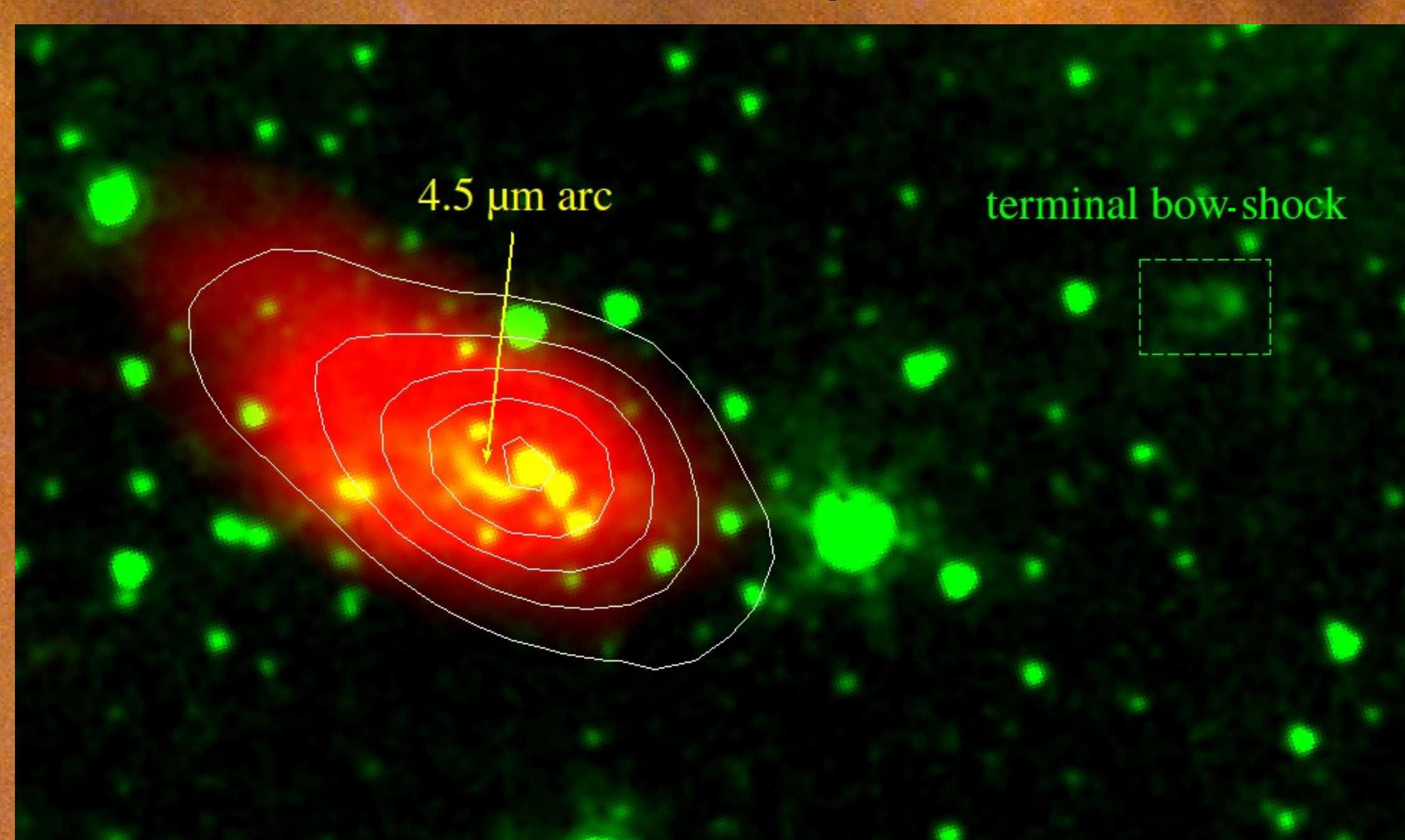


Figure 3: Composite image showing 4.5 μm (green), $\text{HCO}^+(3-2)$ line emission (red), and 870 μm emission from ATLASGAL (in contours). Contours correspond to 0.3 to 1.1 Jy beam $^{-1}$ in steps of 0.2 Jy beam $^{-1}$.

Table 1: Parameters of the newly detected molecular outflow

Parameters	Value
Velocity range of the outflow = v [km s^{-1}]	(−13.5, −8.2)
Maximal velocity = v_{max} [km/s]	7.5
Size of the outflow = l_{CO} [pc]	1.4
Integrated outflow emission in $^{12}\text{CO}(3-2)$ [K km s^{-1}]	5.7
Molecular mass in the blue outflow = M_{H_2} [M_\odot]	13
Momentum in the blue outflow = p [$M_\odot \text{ km s}^{-1}$]	109.2
Mechanical energy = E_K [erg]	9.12×10^{45}
Time scale = r [yr]	1.35×10^5
Mass entrainment rate = \dot{M} [M_\odot/yr]	9.6×10^{-5}
Mechanical force = F_m [$M_\odot \text{ km s}^{-1}/\text{yr}$]	8.09×10^{-4}
Mechanical luminosity = L_m [L_\odot]	0.54

Observations

• **GEMINI observations:** The H_2 (2.122 μm) and K (2.200 μm) images were obtained with the NIR Gemini South Adaptive Optics Imager (GSAOI) and the Gemini Multi-conjugate Adaptive Optics System (GeMS), at Gemini South Telescope, at Cerro Pachón, Chile. They were processed and combined using the THELI program (Schirmer 2013; Erben et al. 2005). The final images have a resolution of 0.09 arcsec pixel $^{-1}$.

• **APEX observations:** The $^{12}\text{CO}(3-2)$ (at 345.796 GHz), $^{13}\text{CO}(3-2)$ (at 330.588 GHz), $\text{C}^{18}\text{O}(3-2)$ (at 329.330 GHz) and $\text{HCO}^+(3-2)$ (at 267.557 GHz) molecular data were observed with the 12 m Atacama Pathfinder EXperiment (APEX) telescope, located in the Llano de Chajnantor, in the Puna de Atacama, Chile. The CO data have an angular resolution of 18'', and the HCO^+ data, 25''. The velocity resolution is 0.3 km s^{-1} .

• **Data bases:** *Spitzer* image at 4.5 μm and APEX Telescope Large Survey of the Galaxy (ATLASGAL) data at 870 μm .

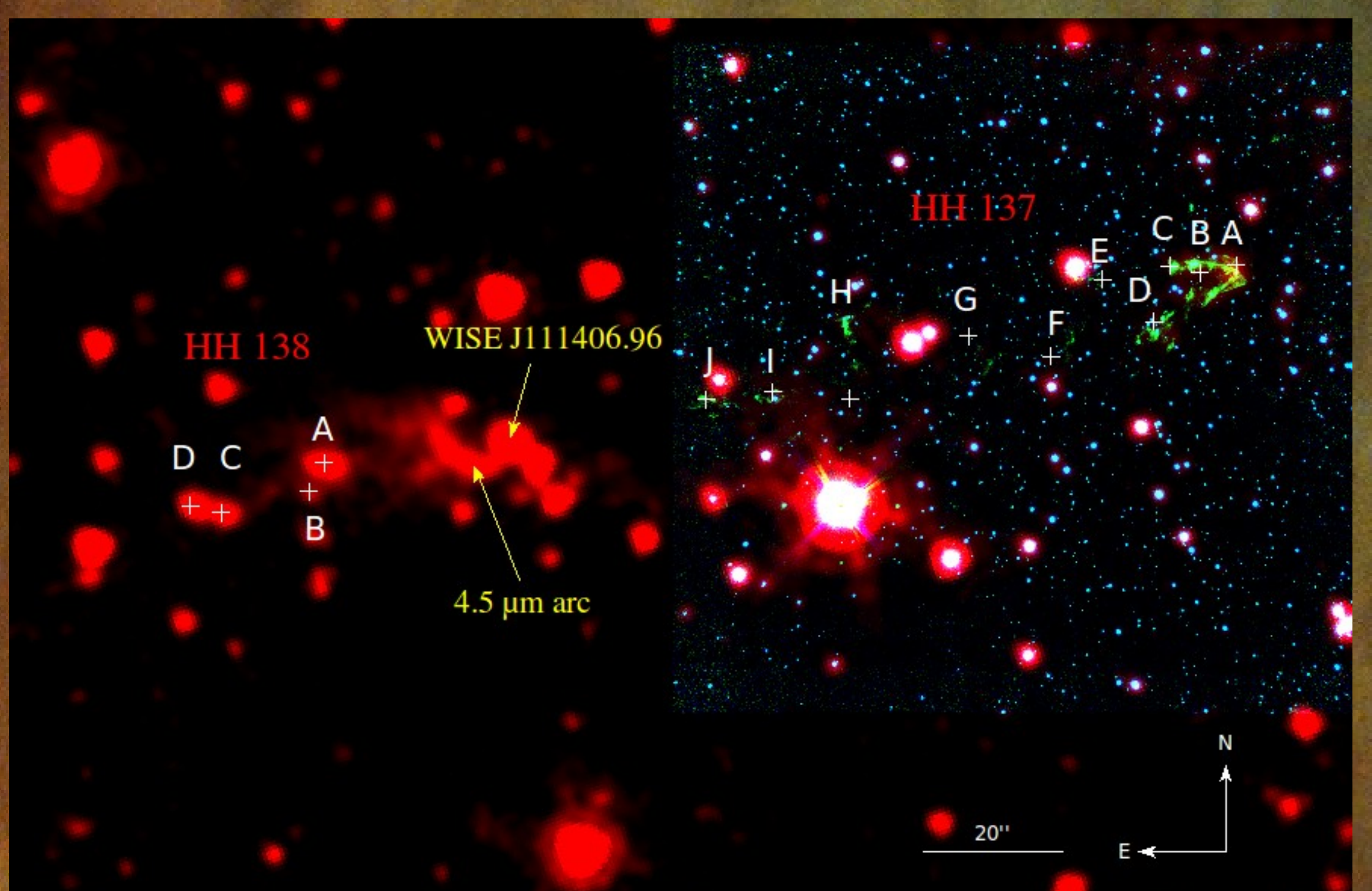


Figure 1: Composite image of HH 137 and 138 showing K (blue) and H_2 (green) taken with GSAOI+GeMS, and 4.5 μm (red) from *Spitzer*. The crosses mark the position of Ogura's knots. The location of the arc-shape structure and the proposed powering source for HH 137 are also marked. Note that the field covered by the Gemini images is much smaller than the *Spitzer* field.

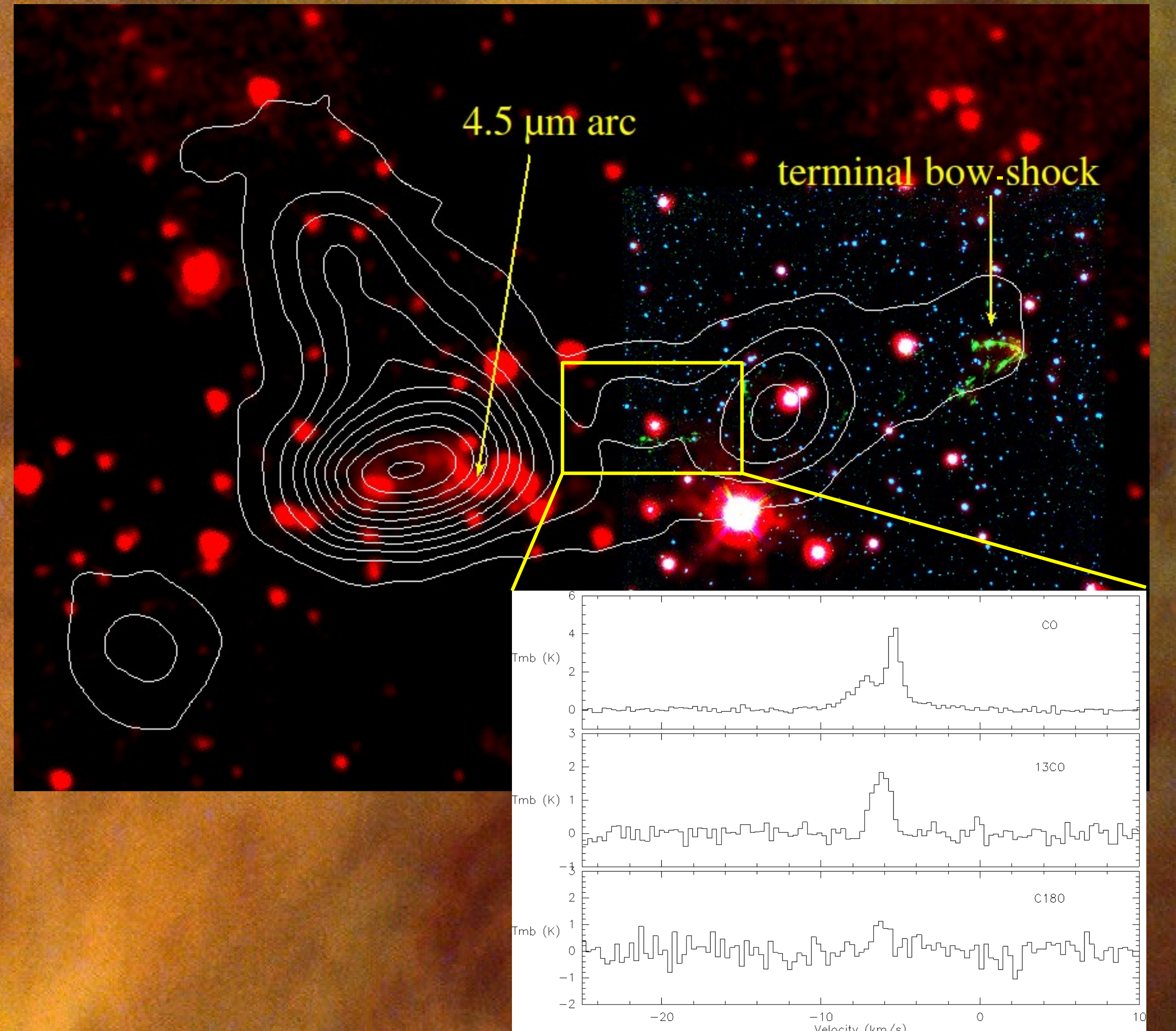


Figure 2: Composite image showing K (blue), H_2 (green), 4.5 μm (red), and the $^{12}\text{CO}(3-2)$ line emission distribution in the interval $[-13.3, -8.4]$ km s^{-1} (in contours). Contour lines correspond to 0.6, 1.2, 1.9, 2.6, 3.1, 3.9, 4.5, 5.2, 5.9, 6.5, 7.1, 7.8, 8.5 and 9.1 K. The lower image shows the $^{12}\text{CO}(3-2)$, $^{13}\text{CO}(3-2)$, and $\text{C}^{18}\text{O}(3-2)$ (amplify by 2) averaged profile in the marked region.

Scenario

We propose a scenario in which the identified YSO drives the blue-shifted lobe of a molecular outflow linked to HH 137. A redshifted lobe of the outflow was not identified using the present data.

We believe that the arc detected at 4.5 μm is the result of the jet colliding with the dense molecular clump. Part of this material could be deflected by the densest part of the cloud, emerging from it and originating the HH 138 knots.

We wonder if the molecular gas extending towards the North in Figure 2 is part of a molecular outflow deflected by the 4.5 μm arc in the region of the dense clump.

References

- Beuther, H., Schilke, P., Sridharan, T. K., et al. 2002, *A&A*, 383, 892
- Bronfman, L., Garay, G., Merello, M., et al. 2008, *ApJ*, 672, 391
- Buckle, J. V., Curtis, E. I., Roberts, J. F., et al. 2010, *MNRAS*, 401, 204
- Chen, X., Shen, Z.-Q., Li, J.-J., Xu, Y., & He, J.-H. 2010, *ApJ*, 710, 150
- Csengeri, T., Urquhart, J. S., Schuller, F., et al. 2014, *A&A*, 565, A75
- Erben, T., Schirmer, M., Dietrich, J. P., et al. 2005, *Astronomische Nachrichten*, 326, 432
- Hartley, M., Tritton, S. B., Manchester, R. N., Smith, R. M., & Goss, W. M. 1986, *A&AS*, 63, 27
- Koenig, X. P., Leisawitz, D. T., Benford, D. J., et al. 2012, *ApJ*, 744, 130
- Ogura, K. 1993, *MNRAS*, 262, 735
- Reach, W. T., Rho, J., Tappe, A., et al. 2006, *AJ*, 131, 1479
- Schirmer, M. 2013, *ApJS*, 209, 21
- Schuller, F., Menten, K. M., Contreras, Y., et al. 2009, *A&A*, 504, 415
- Smith, M. D. & Rosen, A. 2005, *MNRAS*, 357, 1370
- Targon, C. G., Rodrigues, C. V., Cerqueira, A. H., & Hickel, G. R. 2011, *ApJ*, 743, 54
- Tóth, L. V., Marton, G., Zahorecz, S., et al. 2014, *PASJ*, 66, 17
- Watson, C., Hanspal, U., & Mengistu, A. 2010, *ApJ*, 716, 1478